

Theoretical XANES spectra for C_{76} isomers^{*}

ZHAO Ting(赵挺)¹ GAO Bin(高斌)¹ LIU Lei(刘蕾)¹ YE Qing(叶青)¹
CHU Wang-Sheng(储旺盛)¹ WU Zi-Yu(吴自玉)^{1,2,3;1)}

1 (Beijing Synchrotron Radiation Facility, Institute of High Energy Physics, CAS, Beijing 100049, China)

2 (National Synchrotron Radiation Laboratory, University of Science and Technology of China, Hefei 230026, China)

3 (Theoretical Physics Center for Science Facilities, Chinese Academy of Sciences, Beijing 100049, China)

Abstract Two isolated pentagon rule satisfying isomers of C_{76} are optimized. And $1(D_2)$ isomer is reconfirmed to be the relative more stable one. The X-ray absorption near-edge structure (XANES) spectra are theoretically characterized by the hybrid density functional theory (DFT) method in combination with the full core-hole potentials. Isomer identification of XANES spectra for C_{76} is found and XANES spectra dependence on local structure of fullerene is discussed.

Key words fullerene C_{76} , isomer, calculated XANES spectra, local structure dependence

PACS 33.20.Rm, 31.15.es, 41.60.-m

1 Introduction

The discovery of C_{60} ^[1] — the first molecular allotropes of carbon, lifting the curtain on intensive researches for fullerene family, resulted in the boom of isolation, macroscopical production and configurable characterization of various carbon cages with different molecular weights. The development of fullerenes profoundly influenced all aspects of contemporary carbon chemistry. Moreover the functionalization of the carbon cages, such as enclosing metal and doping non-metal^[2–5], led to numerous new molecular structures that are continuously investigated for their fundamental physicochemical properties, as well as for the application in advanced materials.

With increasing size, the number of fullerene isomers rapidly multiplies, and as a consequence of the hypothesis that adjacent fivemembered rings within a fullerene cage would produce structures of higher energy, most of the experimentally isolated fullerenes are part of a subset satisfying the isolated pentagon rule (IPR)^[6]. The present paper focuses on C_{76} , which is the first fullerene possessing more than one IPR-satisfying isomer—exactly two with D_2 symmetry and T_d symmetry respectively. The D_2 isomer has been isolated and characterized^[7], whereas the T_d isomer has never been observed experimentally.

However, isomer sensitivity of spectra by calculation is fundamentally interesting and stimulating for the experimental research^[8–10]. In this work, the geometries of the two IPR-satisfying isomers of C_{76} were optimized using ab initio B3LYP/6-31G(d, p) method. Then, based on the optimized structures, the X-ray absorption near-edge structure (XANES) spectra were calculated with the gradient-corrected density functional theory and Spectral identification of the two C_{76} isomers was discussed. Finally, explorations of the local-environment dependence for the XANES spectra of fullerenes were conducted.

2 Structure optimization

The geometries of the two isomers of C_{76} were optimized at B3LYP level with 6-31G(d, p) basis set as implemented in the GAUSSIAN 03 program^[11]. The structures of both isomers are found to correspond to local minimums on a potential energy surface and are expected to be stable once they are formed. However, the symmetry of Th isomer could not be maintained but lowers to D_{2d} because of the Jahn-Teller distortion^[6, 12]. In Fig. 1, the ultima equilibrium structures of the two isomers are displayed. The results of our calculation are qualitative coincidence with the formers^[13–16]: $1(D_2)$ isomer has a

Received 17 December 2008, Revised 31 March 2009

* Supported by Knowledge Innovation Program of Chinese Academy of Sciences

1) E-mail: wuzy@ustc.edu.cn

©2009 Chinese Physical Society and the Institute of High Energy Physics of the Chinese Academy of Sciences and the Institute of Modern Physics of the Chinese Academy of Sciences and IOP Publishing Ltd

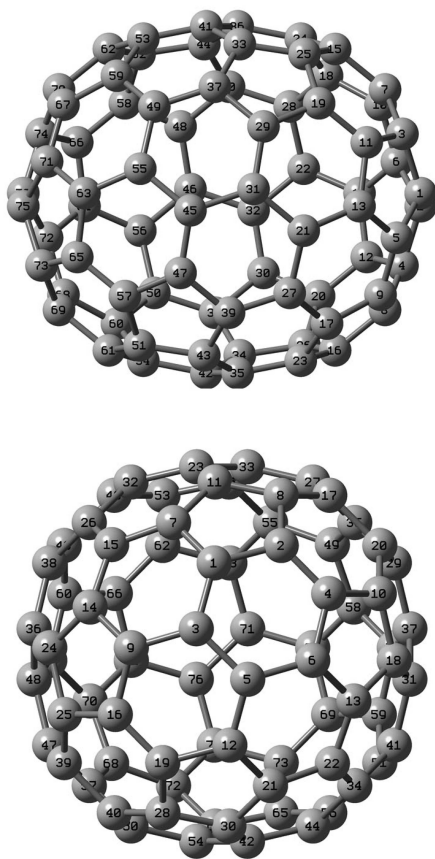


Fig. 1. The equilibrium structure of C₇₆ isomers: 1(D₂) (upper) and 2(Td→D_{2d}) (lower). The pellets represent the C atoms and the sticks represent the covalent bands between C atoms. The nomenclature for isomers is in conformity with that given in Ref. [6]. For 1(D₂) isomer, there are 19 symmetry independent C atoms labeled as 1, 3, 5, 7, 9, 11, 13, 15, 17, 19, 21, 23, 25, 27, 29, 31, 33, 35, 37; while for 2(Td→D_{2d}) isomer, 11 symmetry independent C atoms labeled as 1, 2, 3, 4, 6, 7, 8, 11, 13, 15, 23.

lower total energy and a larger LUMO-HOMO gap, explaining the favored existence of 1(D₂) in the experiment. At the same time, quantitative parameters are discrepant because of different arithmetic or base sets. For the convenience of contrast, a relative energy of the results together with LUMO-HOMO gaps by different theoretical methods, are given in Table 1.

As will be discussed below, carbon atoms of the fullerenes can be classified into three sorts according to the local environment^[9]: (1) the pyracylene site, where the carbon atom lying in a pentagon is joined through an exo bond to another pentagon, (2) the corannulene site, where the carbon atom lying in a pentagon ring is joined through an exo bond to a hexagon, and (3) the pyrene site, where the carbon is part of three hexagons. The pyracylene and corannulene sites originate from C₆₀, while the pyrene site is introduced by the extra carbon atoms that have been added to the C₆₀ molecule to form the larger fullerene. The different combinations of the pyracylene and corannulene sites conduce to the different isomers. At the mention of C₇₆, there are 36 pyracylene sites and 24 corannulene sites for 1(D₂), 24 pyracylene sites and 36 corannulene sites for 2(Td→D_{2d}).

3 Theoretical methods for XANES

The XANES technique as an atomic selective method^[17, 18] involves the excitation of core electrons into unoccupied orbitals. It is thus a probe for the unoccupied valence energy levels. The theoretical XANES spectra, obtained by computing the transition dipole moment from the C 1s to the unoccupied orbitals, were carried out using the code StoBe^[19] with the gradient corrected Becke (BE88) exchange functional^[20] and the Perdew (PD86) correlation functional^[21] on the basis of optimized

Table 1. The energies (kcal/mol) of the 2(Td→D_{2d}) relative to 1(D₂) for fullerene C₇₆ and LUMO-HOMO gaps (eV) calculated by different theoretical methods.

	HF/ STO-3G ^[a]	HF/ double- ζ ^[b]	TBMD ^[c]	QCFF/PI ^[d]	PM3 ^[e]	TBMC ^[f]	B3LYP/6-31G*// HF/3-21G ^[g]	B3LYP/ 6-31G(<i>d,p</i>) ^[h]
ΔE	45.4	42.7	5.3	59	25.28	6.19	17.47	14.48
LUMO-HOMO gap of 1(D ₂)			0.796	5.2				1.98
LUMO-HOMO gap of 2(Td→D _{2d})			0.096	4.1				0.831

[a] Hartree-Fock self-consistent field level of theory employing STO-3G basis sets^[13]. [b] Hartree-Fock self-consistent field level of theory employing double- ζ basis sets^[13]. [c] Tight-binding molecular dynamics method^[14]. [d] Semi-empirical QCFF/PI methods^[15]. [e] Semi-empirical PM3 method^[16]. [f] Tight-binding Monte Carlo method^[16]. [g] Geometries optimized at HF/3-21G level and energies computed at B3LYP/6-31G*^[16]. [h] Our method: B3LYP/6-31G(*d,p*) level for both geometries optimizing and energies computing.

structures. The IGLO-III basis set of Kutzelnigg et al.^[22] was used to describe the core-excited atoms, and four electron effective core potentials for the remaining atoms. We employed a full core-hole (FCH) potential method in combination with a double-basis-set technique, where a normal orbital basis set was used for the minimization of the energy, and an augmented diffuse basis set^[23] ($19s,19p,19d$) for the computation of the transition moments and excitation energies of core-excited states. The full core-hole potential gives excellent XANES intensities as well as good relative energy positions for similar systems^[8–10]. In order to obtain absolute energy positions of the peaks, the energy levels were calibrated according to the Δ Kohn-Sham (Δ KS) calculations, so that the first spectral feature, corresponding to the transition to the lowest unoccupied orbital (LUMO) coincided with the calculated excitation energy of the C1s to the LUMO. Ionization potentials (IP's) were also computed using the Δ KS scheme, that is, as the energy difference between the ground state and the fully optimized core-ionized state. Relativistic effects of 0.2 eV for the carbon K -edge^[24] were also taken into account to produce the overall shift of the spectrum. The XANES spectra were finally formed by using a

Gaussian function with full width at half maximum (FWHM) of 0.5 eV in order to convolute the oscillator strengths below the IP, while a Stieltjes imaging approach^[25] in the continuum, above the IP.

4 Results and discussion

The carbon K -edge XANES spectra of both isomers, together with corresponding components for the three different types of carbon atoms are shown in Fig. 2. Dramatic differences both on profiles and peak positions are exhibited for the two isomers. For a detailed contrast, we focus on the range between 283 and 286 eV^[9] with accurate energy positions of the three peaks as shown in Table 2. In both cases Peak C is the most intensive one, whereas the relative intensities of Peak A and B are contrary. All the three peaks in $2(Td \rightarrow D_{2d})$ seem to shift toward a lower energy by about 0.5–0.7 eV. Compared with those in $1(D_2)$, the energy separation between Peak A and C is 1.6 eV, being similar in the two spectra. The specific profiles for the two XANES spectra provide an efficacious approach to discern the fullerene isomers.

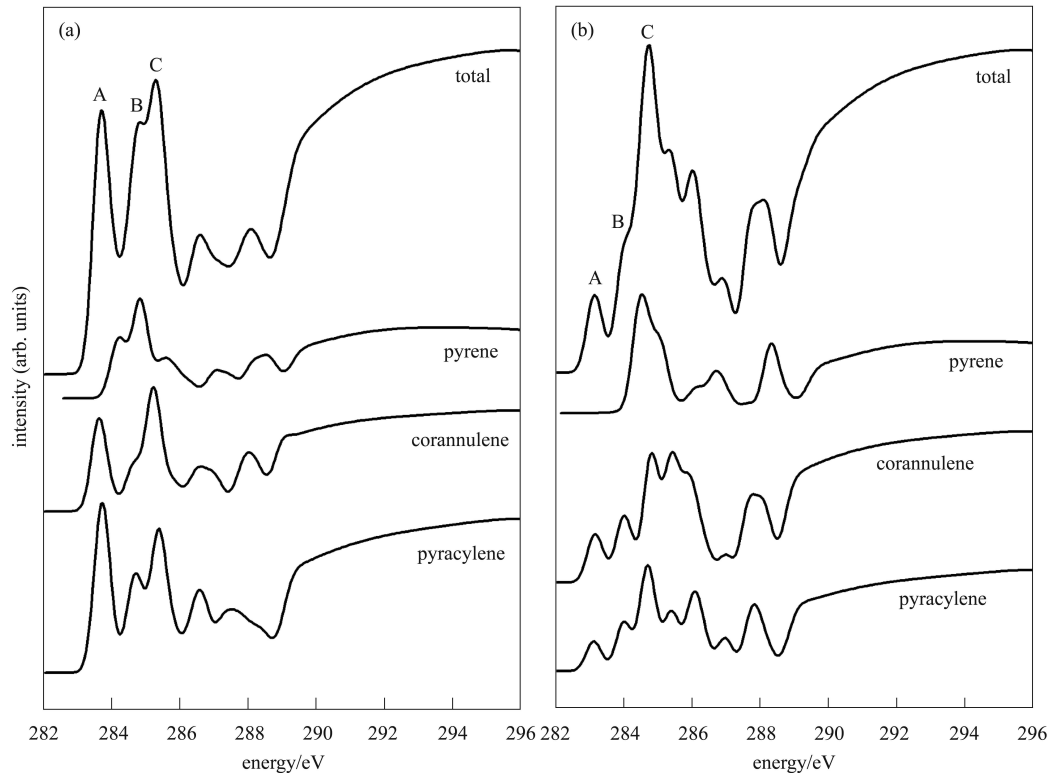


Fig. 2. The calculated carbon K -edge XANES spectra of the isomers (a) $1(D_2)$ and (b) $2(Td \rightarrow D_{2d})$ with corresponding components for the three different sites of carbon atoms. The spectra are obtained by computing the XANES spectra for the symmetry independent atoms and summing up the different contributions scaled with the relative abundance of every site of carbon atoms.

Table 2. The energy positions (eV) of the peaks in XANES spectra for isomers 1(D_2) and 2($Td \rightarrow D_{2d}$) range between 283 and 286 eV.

system	A	B	C
1(D_2)	283.69	284.84	285.29
pyrene	284.23	284.83	285.58
corannulene	283.64	284.64	285.24
pyracylene	283.76	284.71	285.41
2($Td \rightarrow D_{2d}$)	283.15	284.10	284.75
pyrene		284.55	285.00
corannulene	283.17	284.02	284.82
pyracylene	283.10	284.00	284.70

The provenance of these peaks can be analyzed by the decomposed spectra of three sorts of carbon atoms mentioned above. From Fig. 2, one can see clearly that, for both isomers, Peak A and Peak C significantly originate from the carbons of corannulene site and pyracylene site while the ones of pyrene site

mainly construct Peak B. This is coincidental with Refs. [9] and [10], thus confirming Peak B to be the fingerprint of the special fullerene isomer.

Hereto, the XANES spectra of C_{70} , C_{76} , C_{78} , C_{80} , and C_{82} have been calculated and discussed using the same theoretical method. For all the cases, the XANES spectra, with the second peak primarily stemming from excitations of the pyrene component universally, suffice for fullerene isomer identification. On the other hand, besides the fingerprint peak, the evolvement of XANES spectra for fullerene series hardly shows any other commonness. The spectra vary from fullerene to fullerene and no uniform features are exhibited to distinguish fullerenes with specific number of carbon atoms. This can be easily understood by the fact that the XANES technique is sensitive to the local atomic and electronic structure of the adsorbing element, which is different for fullerenes with different sizes.

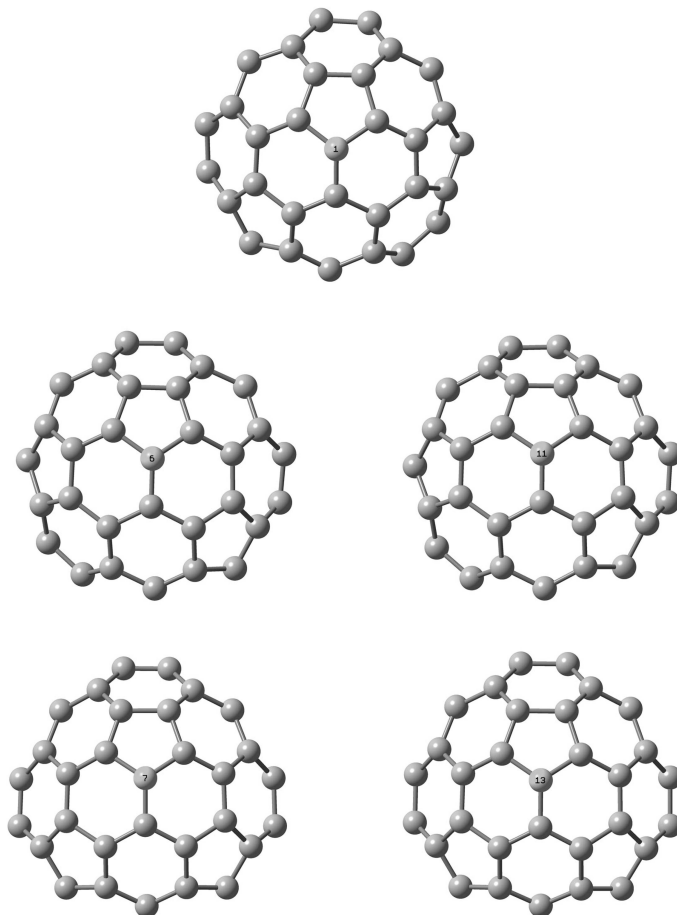


Fig. 3. Local structures for five symmetry independent C atoms (labeled as 1, 6, 7, 11, 13) at corannulene sites of isomer 2($Td \rightarrow D_{2d}$). The tabs are consistent with those in Fig. 1. According to the different permutations of the pentagons and hexagons in the second layer, Atom 6 and 11 are of the same kind, namely Group I; Atom 7 and 13 belong to another kind, namely Group II. The permutation of the pentagons and hexagons in the second layer for Atom 1 is the enantiomorphism of that for Atom 6 (or 11). So Atom 1 is equivalent in XANES to Atom 6 (or 11), and can therefore belong to Group I.

In the following work, to illustrate the exact dependence of XANES spectra on the local structures of fullerenes, the spectra for the two isomers of C_{76} are investigated in a more delicate way. We further explore the spectra of carbon atoms in the same site classified above. It is noticeable that the decomposed XANES spectra of $1(D_2)$, are not accordant with the counterparts of $2(Td \rightarrow D_{2d})$, and also one should be aware that the forenamed classification of carbon atoms does not distinguish all the symmetry independent atoms. A thorough scan of the more idiographic carbon atoms will reveal more abundant information for the XANES spectra.

We ulteriorly sort each site of carbon atoms by not only considering the first layer of polygons (pentagons and hexagons) around the exact carbon atom, but also the second layer.

In the case of $2(Td \rightarrow D_{2d})$ isomer, there are 36 carbon atoms falling into corannulene sites, with only five of those symmetrically discernable, which are labeled as 1, 6, 7, 11 and 13 in Fig. 3. All the five carbon atoms identically lie at the juncture of one pentagon and two hexagons, nevertheless when the outer layer which contains 2 pentagons and 6 hexagons is taken into account, two kinds of carbon sites, namely Group I and II, are exhibited with the different permutations of the pentagons and hexagons (Fig. 3). The individual XANES spectra for the corresponding carbon atoms at corannulene sites are illustrated in Fig. 4, with the accurate energy positions of the peaks listed in Table. 3. Visibly, the spectra of the corannulene 1, 6, and 11 in Group I show great similarity both in the spectral profiles and the peak positions; and it is the same for Corannulene 7 and 11 in Group II. However, for different groups, distinct features exist in the range between 285 and 287 eV. It is thus indicative that the XANES spectra of the carbon atoms in fullerenes are mainly determined by the primal two layers of polygons around them.

Comparison among the individual XANES spectra for carbon atoms at pyrene and pyracylene sites

of $2(Td \rightarrow D_{2d})$ is also made respectively, as described in Fig. 5. The similarity for the spectra at pyracylene sites, corresponding to 2, 4, 8, implies the same permutation of the pentagons and hexagons for the first two layers, while the three symmetry independent carbon atoms tagged as 3, 15, 23 belong to two groups according to their XANES spectra. Those conjectures are consistent with the results given by the optimized structure for $2(Td \rightarrow D_{2d})$ (Figure is elided). In addition, even the carbon atoms in the same group classified at the more delicate level show distinction in relative intensity for the XANES spectra. This may result from the polygons of outer layers or the diversity of local curvature for each site. Also mentioned are the XANES spectra for individual carbon atoms of $1(D_2)$ isomer, which show over again that the spectra are sensitive to the first two layers of pentagons around the corresponding carbon atoms. In spite of that, due to the ellipsoid shape of $1(D_2)$ (Fig. 1), the tortuosity is widely discrepant at different positions, and so the XANES spectra for the same kind of carbon atoms with two surrounding layers considered show a little bigger deviation than those for $2(Td \rightarrow D_{2d})$.

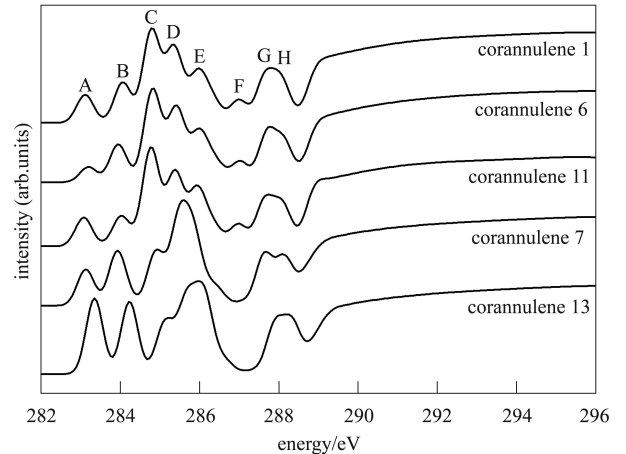


Fig. 4. The individual XANES spectra for the symmetry independent C atoms at corannulene sites of isomer $2(Td \rightarrow D_{2d})$.

Table 3. The energy positions (eV) of the peaks in XANES spectra for the symmetry independent C atoms at corannulene sites of isomer $2(Td \rightarrow D_{2d})$.

	A	B	C	D	E	F	G	H
corannulene 1	283.11	284.06	284.78	285.34	285.97	286.97	287.79	287.9
corannulene 6	283.17	283.94	284.80	285.42	286.00	286.99	287.79	287.96
corannulene 11	283.08	284.02	284.76	285.39	285.92	286.96	287.72	287.99
corannulene 7	283.13	283.93	284.92	285.61			287.69	288.09
corannulene 13	283.35	284.23	285.20	286.00			288.02	288.2

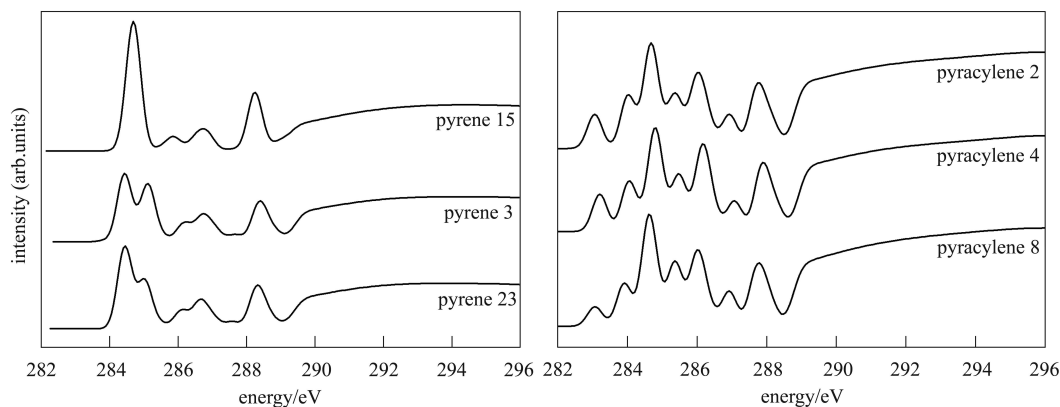


Fig. 5. The individual XANES spectra for the symmetry independent C atoms at pyrene (left) and pyracylene (right) sites of isomer 2(Td→D_{2d}). Pyrene 3 and 23 remain with one group while Pyrene 15 another; all C atoms at pyracylene sites are of the same group, according to the spectral similarity.

5 Summary

Herein, we have theoretically calculated the XANES spectra for IPR-satisfying isomers of C₇₆. The corresponding components of XANES spectra for the three different sites of carbon atoms shed light on the origination of peaks in the total spectra. And

the differences between the spectra enable an effective method to identify the two isomers. Analyzing individual spectra for the C atom of C₇₆ reveals that the individual spectra are mainly determined by the primal two layers of polygons around the carbon atom and could be affected by the geometry around.

References

- Kroto H W, Heath J R, O'Brien S C et al. *Nature (London)*, 1985, **318**: 162—163
- Nishibori E, Takata M, Sakata M et al. *Angew. Chem. Int. Ed.*, 2001, **40**: 2998—2999
- Yamada M, Nakahodo T, Wakahara T et al. *J. Am. Chem. Soc.*, 2005, **127**: 14570—14571
- Stevenson S, Rice G, Glass T et al. *Nature*, 1999, **401**: 55—57
- Saunders, Jiménez-Vázquez H A, Cross R J et al. *Science*, 1993, **259**: 1428—1430
- Fowler P W, Manolopoulos D E. *An Atlas of Fullerenes*. London: Clarendon Press, 1995. 68—93
- Ettl R, Chao I, Diederich F. *Nature*, 1991, **353**: 149—152
- Brena B, LUO Y. *J. Chem. Phys.*, 2003, **119**: 7139—7144
- Bassan A, Nyberg M, LUO Y. *Phys. Rev. B*, 2002, **65**: 165402
- GAO Bin, LIU Lei, WU Zi-Yu et al. *J. Chem. Phys.*, 2007, **127**: 164314
- Frisch M J, Trucks G W, Schlegel H B et al. *GAUSSIAN 03*, Revision D.01, Gaussian, Inc., Wallingford CT, 2004
- Kroto H W. *Nature*, 1987, **329**: 529—531
- Colt O R, Scuseria G E. *J. Phys. Chem.*, 1992, **96**: 10265—10268
- ZHANG B L, WANG C Z, HO K M. *Chem. Phys. Lett.*, 1992, **193**: 225—230
- Austin S J, Fowler P W, Orlandi G. *Chem. Phys. Lett.*, 1994, **226**: 219—225
- LIN Yi, CAI Wen-Sheng, SHAO Xue-Guang. *Journal of Molecular Structure: THEOCHEM*, 2006, **760**: 153—158
- LEE P A et al. *M. Rev. Mod. Phys.*, 1981, **53**: 769—806
- Kuniko H et al. *J. Am. Chem. Soc.*, 2004, **126**: 15618—15623
- StoBe-deMon version 2.2. 2006, Hermann K, Pettersson L G M, Casida M E, Daul C, Goursot A, Koester A, Proynov E, St-Amant A, Salahub D R. Contributing authors: Carravetta V, Duarte H, Friedrich C, Godbout N, Guan J, Jamorski C, Leboeuf M, Leetmaa M, Nyberg M, Patchkovskii S, Pedocchi L, Sim F, Triguero L, Vela A
- Becke A D. *Phys. Rev. A*, 1988, **38**: 3098—3100
- Perdew J P. *Phys. Rev. B*, 1986, **33**: 8822—8824
- Kutzelnigg W, Fleischer U, Shindler M. *NMR-Basic Principles and Progress*. Heidelberg: Springer-Verlag, 1990. Vol. 23, p. 165
- Triguero L, Pettersson L G M, Ågren H. *Phys. Rev. B*, 1998, **58**: 8097—8110
- Triguero L, Plashkevych O, Pettersson L G M. *J. Electron Spectrosc. Relat. Phenom.*, 1999, **104**: 195—207
- Langhoff P W. *Electron-Molecule and Photon-Molecule Collisions*. New York: Plenum Press, 1979. 98—155